Inorganic Chemistry

Article

pubs.acs.org/IC

Synthesis and Visible-Light Photochromism of a New Composite Based on Polymolybdate Enclosed in Magadiite

Yufeng Chen,* Gensheng Yu, and Fei Li

Department of Chemistry, Nanchang University, Jiangxi Province, 330031 People's Republic of China

Michael Severance

Department of Chemistry, The Ohio State University, Columbus, Ohio 43210, United States

ABSTRACT: A new composite based on polymolybdate incorporated in layered magadiite has been synthesized via a exfoliation/self-assembly process. Various techniques, including X-ray diffraction (XRD), X-ray photoelectron spectroscopy (XPS), scanning electron microscopy coupled with energy-dispersive X-ray analysis (SEM-EDX), Raman spectroscopy, thermogravimetric (TG) analysis, UV−vis spectroscopy, and transmission electron microscopy (TEM), have been employed to characterize the composite. Results indicated that the polymolybdate particles were incorporated into the layered magadiite. Upon the irradiation of visible light (420−630 nm), the composite changed color from yellow to dark blue; moreover, the color can be bleached upon exposure to a 15% H_2O_2 solution. The visible-light illumination and H_2O_2 treatment can be repeated in excess of 10 times. The mechanism of photochromism has been investigated, and the reversibility is attributed to the hydration property of host magadiite and oxidative ability of H_2O_2 solution.

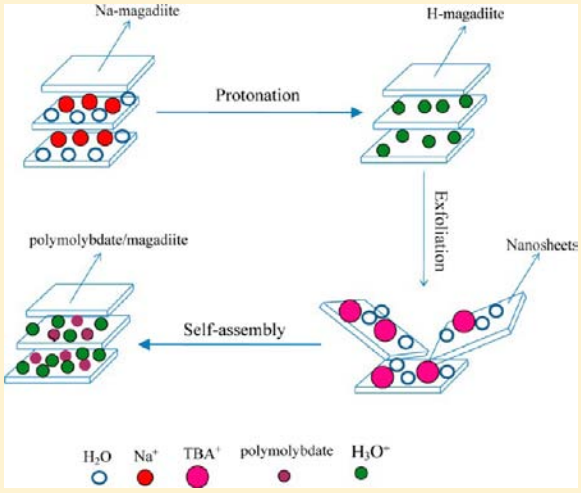

INTRODUCTION

Photochromic materials have received much attention for more than three decades, because of their potential industrial applications as optical power-limiting switches, optical information storage, smart painting, etc.[1] Although less extensively investigated than organic photochromic materials or organic−inorganic hybrid materials,[2] inorganic or inorganic−inorganic composite photochromic materials (such as polymolybdates) are still considered to be promising photochromic materials with higher thermal stability .

The photochromic behavior of amine molybdates in the solid state was first noticed in piperidinium molybdates, which changed color from white to pink-brown upon sunlight irradiation.[1a] Some alkylammonium polyoxomolybdates, including the secondary and tertiary ammonium polyoxomolybdates, can be colored upon ultraviolet (UV) irradiation at wavelengths corresponding to the O → Mo LMCT transition (<400 nm).[3] The colored polyoxomolybdates can return to their original color in the presence of oxygen in darkness. Moreover, it was found that the water molecules play an important role in the photochromism of molybdenum compounds.[4] Although many studies on photochromic properties of molybdenum compounds have been reported, some important questions are left unanswered. For instance, most studies on the photochromism of molybdenum oxide or molybdate are based on UV light irradiation, while there are few studies focusing on visible-light photochromism. Moreover, the reversibility of photochromic polymolybdates under visible-light irradiation is hardly reported.

Based on the above discussion, we examine the host magadiite for polymolybdate encapsulation and the oxidant H_2O_2 for the bleaching for visible-light irradiated polymolybdate in the present work. Magadiite ($Na_2Si_{14}O_{29}\cdot xH_2O$) is a layered structure with good hydration properties (it has the ability to store water molecules).[5] It has a multilayered silicate structure composed of two-dimensional (2D) units of host layers and guest cations that exist between the layers.[6] It is attractive as a host material, because it exhibits a broad range of properties, including adsorption, intercalation, exfoliation, and organization of guest species.[7] A H_2O_2 solution has been used as a bleaching agent for the Methyl Orange catalyzed by MoO_4^{2-} and WO_4^{2-}.[8] The role of H_2O_2 in the present work is that it not only can bleach colored polymolybdate, but it can also supply water molecules to host magadiite. We report that the composite based on polymolybdate enclosed in magadiite exhibits good photochromic properties under visible-light irradiation, which can be reversed by hydrogen peroxide oxidation. This cycle can be repeated in excess of 10 times.

Received: January 22, 2013
Published: June 13, 2013

   dx.doi.org/10.1021/ic400569y | *Inorg. Chem.* 2013, 52, 7431−7440

Table 1. Chemical Composition of Na-Mag and Polymolybdate/Mag Composite

	Composition (%)							
	Na	Mo	Si	O	C	H	N	H_2O^a
Na-Mag Sample, Chemical Formula: $Na_{2.0}Si_{13.8}O_{28.6}\cdot 7.0H_2O$								
calculated[b]	4.53		38.03	56.06		1.38		12.40
found[b]	4.52		37.98	56.01		1.43		12.43
Polymolybdate/Mag Sample, Chemical Formula: $H_{2.0}Si_{13.9}O_{28.8}/[TBA_{1.8}H_{2.2}\cdot(Mo_8O_{26})]_{0.2}\cdot 2.7H_2O$								
calculated[b]		12.53	31.78	47.94	5.64	1.70	0.41	4.0
found[b]		12.51	31.75	47.89	5.71	1.76	0.43	4.12

[a] H_2O obtained from TG. [b] Na, Mo, Si, and O analyzed by EDX; C, H, N obtained from CHN elemental analysis.

EXPERIMENTAL SECTION

Materials. Na-magadiite was synthesized via the reaction of SiO_2–NaOH–Na_2CO_3 system under hydrothermal conditions.[9] At 150 °C, the reaction was carried out in a sealed Teflon-lined autoclave containing silica gel solution (15 mL of 40 wt % SiO_2 silica gel and 70 mL of H_2O), NaOH (0.7412 g), and Na_2CO_3 (2.8139 g) as the reactants. After reaction for 96 h, the product was filtered, washed, and dried at 40 °C for 12 h. The obtained Na-magadiite sample was labeled as Na-Mag. The protonation of the Na-Mag (2.4221 g) was performed by soaking in 100 mL of a HCl aqueous solution (0.1 M), stirred for 3 days, and then filtered, washed, and dried at 40 °C in air. The obtained H-magadiite sample was labeled as H-Mag.

A colloidal nanosheet dispersion of exfoliated magadiite was obtained by adding a specific amount of protonated powder (H-Mag, 0.9374 g) in 100 mL of a tetra-*n*-butylammonium hydroxide (TBAOH) aqueous solution (0.1 M), and stirred at room temperature for 5 days. Sodium molybdate solid (0.1677 g) was dissolved in colloidal suspension (9.374 g L^{-1}, 100 mL) of H-Mag. Then, 1.0 M HCl was added dropwise into the mixed solution (pH 11.2), with stirring, and acidified to pH 2. During this process, a colloidal precipitate formed. After the precipitate was filtered, washed with deionized water, and dried at 40 °C for 24 h in air, the final yellow sample was labeled as polymolybdate/Mag.

Characterization. Powder X-ray diffraction (XRD) patterns were collected using a Bruker D8 Focus system (40 kV, 40 mA) with Cu Kα radiation; data acquisition was performed using a scan speed of 2°/min, and 2θ = 3.0°–70°. The Raman spectra were measured with a RENISHAW inVia Raman microscope. The excitation light was the 633-nm line from a He–Ne laser. An environmental scanning electron microscopy (SEM) system that was equipped for energy-dispersive X-ray analysis (SEM-EDX) (Model XL30 ESEM FEG, Philips, Genesis2000, Eindhoven, The Netherlands) was used for the morphological analysis of the surface structure and to determine the elemental composition of the samples. An accelerating voltage of 20 kV and count time of 60 s (peaks) was used for the EDX microanalysis. The *X*-axis of the EDX spectra displays the X-ray energy (in keV); the *Y*-axis reports the intensity of the X-ray signal (counts). X-ray photoelectron spectroscopy (XPS) analysis was performed with a Thermo ESCALAB 250 (V.G. Scientific Co., U.K.) using monochromatic Al Kα radiation (1486.6 ev) as the excitation source. All spectra were acquired at a pass energy of 20 eV with the anode operated at 150 W. Thermogravimetric (TG) analysis data were collected using synchronous thermal analyzer (STA-200, Dazhan, Jiangsu, PRC) under a nitrogen atmosphere at a scan rate of 10 °C/min. The nanosheets of exfoliated magadiite and the polymolybdate particles enclosed in layered magadiite were observed by transmission electron microscopy (TEM) (Model JEM-2010, JEOL). UV–visible absorption spectra were obtained using a Model UV-2501(PC) spectrophotometer.

In order to irradiate and measure the samples conveniently, the polymolybdate/Mag powders were put into a round groove (with a diameter of 0.5 in.) on a sample support. The samples with a diameter of 0.5 in. were illuminated with light from a 300 W mercury arc lamp. The output light passed through a dichroic mirror (420–630 nm), an infrared (IR) filter, and two focusing lenses, finally illuminating the sample. The visible-light intensity irradiating the samples was determined to be 1.0–5.0 mW/cm^2 with a Model 210 power meter.

The coloration–bleaching process is described as follows. Polymolybdate/Mag powder (0.1820 g) was placed into the round groove of the sample support just mentioned above and pressed tightly. The prepared sample used for coloration–bleaching has a diameter of 0.5 in. and a thickness of 0.3 mm. After the sample was irradiated for some time, its surface turned green-blue to dark blue in color. UV–vis spectral measurements then were performed for the colored sample. When bleaching the samples, the 15% H_2O_2 solution (1–2 small drops) was directly added on the colored surface of the samples. As a result, the color faded quickly (within 2 min). The bleached sample was dried at 40 °C for ~10 min in preparation for another coloration.

RESULTS AND DISCUSSION

Chemical Composition Analysis. Since the present polymolybdate/Mag composite was obtained from a pH 2 reaction system, the possible polymolybdate species were analyzed as follows. Many studies have established that, in alkaline or neutral solutions, the tetrahedral orthomolybdate ion (MoO_4^{2-}) is the main species, while in acid solutions, the tetrahedral MoO_4^{2-} ions will be polymerized. There is evidence from pH data for the equilibria:[10]

$$MoO_4^{2-} + H^+ = HMoO_4^-$$

$$7MoO_4^{2-} + 8H^+ = Mo_7O_{24}^{6-} + 4H_2O$$

$$8MoO_4^{2-} + 12H^+ = Mo_8O_{26}^{4-} + 6H_2O$$

At pH 4.8–6.8, $[Mo_7O_{24}]^{6-}$ is formed in solution.[10] At pH 1–3, $Mo_8O_{26}^{4-}$ is the main species.[2a,10,11] After further acidification of the solution, higher polymers may be formed. In this work, therefore, we believe that the $Mo_8O_{26}^{4-}$ species is the primary polymolybdate ion according to the reaction system (pH 2). In consideration of the cations (H^+ and TBA^+) and anions ($Mo_8O_{26}^{4-}$) as well as negatively charged layers of magadiite present in the reaction system, the possible self-assembly process may be

$$TBA^+\text{-magadiite} + H^+ = \text{H-magadiite} + TBA^+$$

$$xTBA^+ + (4 - x)H^+ + Mo_8O_{26}^{4-} \rightarrow (TBA)_xH_{4-x}Mo_8O_{26}$$

During the self-assembling processing, the neutral species $(TBA)_xH_{4-x}Mo_8O_{26}$ may be incorporated in the H-magadiite to form $(TBA)_xH_{4-x}Mo_8O_{26}$/magadiite composite (labeled as polymolybdate/Mag), and the interlayer H^+ ions compensate

dx.doi.org/10.1021/ic400569y | Inorg. Chem. 2013, 52, 7431–7440

the negatively charged layers. Because layered silicates have interlayer silanol groups,[7f] and some hydrogen bonds exist between interlay water or guests and layers in magadiite,[12] it is highly possible that some hydrogen bonds form between the interlayer silanol groups and polymolybdate. Therefore, the association between the polymolybdate and magadiite may result from hydrogen bonding. In addition, the present composite containing polymolybdate shows a yellow color. This yellow color may not be due to host magadiite, because the pure polymolybdate prepared by the same method also has a yellow color. However, different hybrid materials containing $[Mo_8O_{26}]^{4-}$ showed different colors.[11g,h] The exact cause for the present yellow color is complicated and must be studied in future work.

In order to determine the chemical composition of the $(TBA)_xH_{4-x}Mo_8O_{26}$/Mag composite, CHN elemental analyses, SEM-EDX compositional analyses, and thermogravimetry (TG) analysis were employed. The chemical composition of the Na-Mag and polymolybdate/Mag prepared here was obtained by combining the results of CHN elemental analysis (see Table1), SEM-EDX compositional analyses (see Table 1 and Figure 1), and TG analyses (see Figure 2). The SEM-EDX

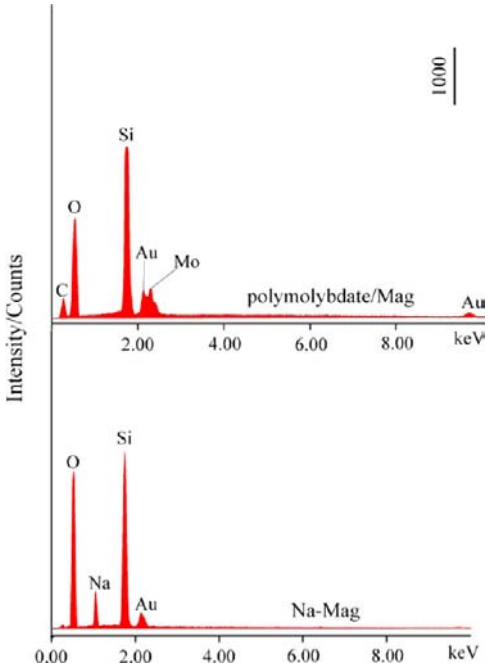

Figure 1. Scanning electron microscopy, coupled with energy-dispersive X-ray spectroscopy (SEM-EDX) results of Na-Mag and polymolybdate/Mag.

compositional analyses revealed the molar ratio of Na:Si:O to be 2.0:13.8:35.6 for the Na-Mag, and the morphological changes of the samples on the basis of SEM images (Figure 3). According to the thermogravimetric curve, Na-magadiite lost 12.4% of its total weight as water below 280 °C, which was mainly due to interlayer water.[13] By combining the EDX analysis, CHN element analysis, and weight loss, as well as the charge-balance principle, an empirical composition for the Na-magadiite prepared was estimated to be $Na_{2.0}Si_{13.8}O_{28.6}\cdot 7H_2O$, which compared favorably with the approximate composition of $Na_2Si_{14}O_{29}\cdot xH_2O$ that was suggested in previous work.[14]

In the light of the calculated value from the chemical formula and the values found from the measurements, the relative errors

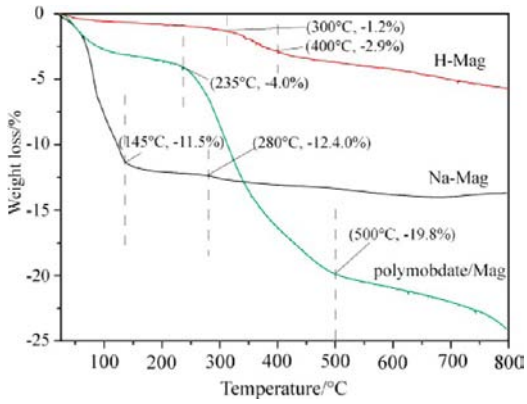

Figure 2. Thermogravimetry (TG) curves of Na-Mag, H-Mag, and polymolybdate/Mag.

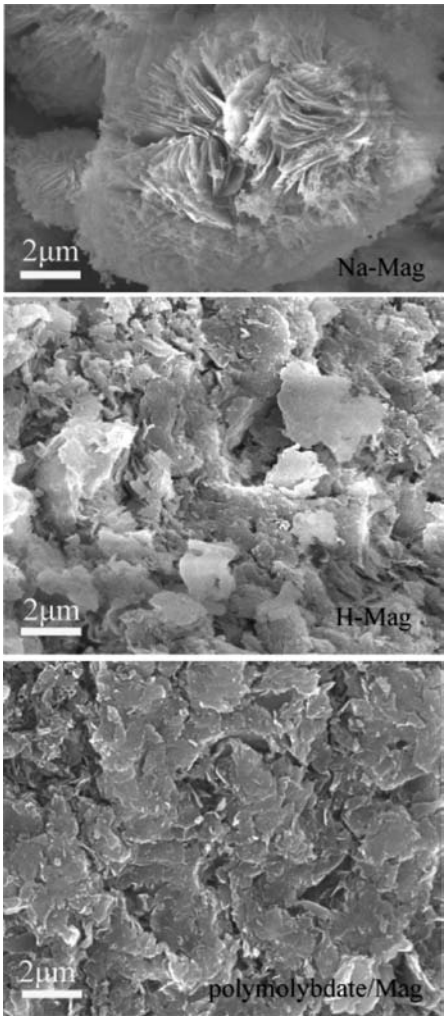

Figure 3. SEM images of Na-Mag, H-Mag, and polymolybdate/Mag.

of elemental Na, Si, and O are −0.22%, −0.13%, and −0.09%, respectively, which are reasonable; while the large error of elemental H is +3.50%, which is due to physically adsorbed water. By the same method, the molar ratio of Mo:Si:O:N:H:C presented in the polymolybdate/Mag composite was estimated to be 1.6:13.9:36.7:0.36:22.6:5.8 and the chemical formula of the composite was estimated to be $H_{2.0}Si_{13.9}O_{28.8}/[TBA_{1.8}H_{2.2}\cdot(Mo_8O_{26})]_{0.2}\cdot 2.7H_2O$, Anal. Calcd (found) (in

dx.doi.org/10.1021/ic400569y | Inorg. Chem. 2013, 52, 7431−7440

wt %): Mo 12.53 (12.51), Si 31.78 (31.75), O 47.94 (47.89), N 0.41 (0.43), H 1.70 (1.76), and C 5.64 (5.71). For elemental Si, Mo, O, C, H, and N, the relative errors are −0.09%, −0.16%, −0.10%, +1.23%, +3.41%, and +4.65%, respectively. The large errors of C and H are due to adsorbed CO_2 and physically adsorbed water, respectively; and the large error of N is due to the small content of nitrogen in the composite. The morphological change from Na-Mag to H-Mag may result from ion-exchange of Na^+ by H^+.

For Na-magadiite, the exchange of Na^+ by a proton is very easy.[15] In the present experimental conditions, the Na^+ was almost exchanged completely by H^+. Since the electronic shell structure and ionic radius of Na^+ and H^+ are different, the structure of magadiite will be changed after the ion exchange of Na^+ by H^+, which was confirmed by XRD result (Figure 4).

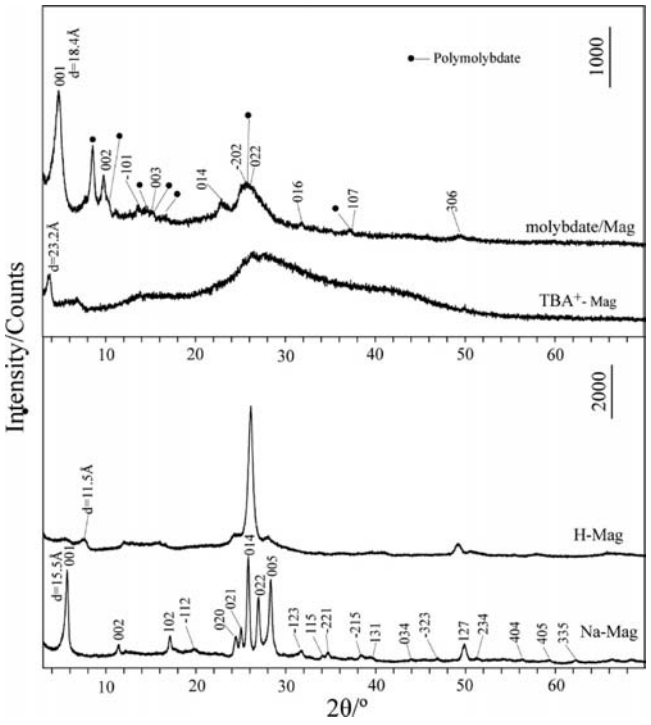

Figure 4. XRD patterns of Na-Mag, H-Mag, TBA^+-Mag, and polymolybdate/Mag.

The structural changes may cause the morphological changes. However, the similar morphology was found between the H-Mag and polymolybdate/Mag composite. This indicated that the layers of magadiite have not been obviously broken during the exfoliation/self-assembly.

For the sake of the confirmation of the composite based on Mo_8O_{26} species incorporated in magadiite, a series of characterization methods, including XRD, Raman spectroscopy, TG, and XPS, were employed as follows.

Powder X-ray Diffraction. The powder XRD pattern of Na-Mag was assigned to the typical layered structure with several (001) reflections corresponding to basal spacing of 15.5 Å.[9,16] All the reflections can be indexed as in Figure 4. The cell parameters of Na-Mag are a = 7.41(1) Å, b = 7.302(2) Å, c = 15.7039(4) Å, and β = 93.585(1)°, which are comparable to the literature values (a = 7.3 Å, b = 7.28 Å, c = 15.71 Å, β = 96.4°).[17] After the reaction of the Na-Mag with HCl, the basal spacing of Na-Mag decreased to 11.5 Å, because of the loss of the interlayer water upon replacement of Na^+ cations by protons. Moreover, except for a strong diffraction peak at $2\theta \approx 26°$, other peaks are very weak, which is consistent with previous reports.[15] When the protonated product (H-Mag) was reacted with tetra-*n*-butylammonium (TBA^+) hydroxide aqueous solution, the powder XRD pattern of TBA^+-Mag exhibited a wavy and broad pattern. Except for a weak d_{001} reflection at 2θ = 3.800° (corresponding to a basal spacing of 23.2 Å), no other reflections were observed. This suggests that the interlayer spacing of magadiite was swollen by the larger TBA^+ group, or even exfoliation of the layered H-Mag by TBA^+ occurred.[16a] By treating the mixed system of TBA^+-Mag and sodium molybdate with HCl solution, followed by water-washing and drying, a well-ordered phase (labeled as polymolybdate/Mag) with a basal spacing of 18.4 Å was obtained. This basal spacing (18.4 Å) was markedly larger than those of H-Mag (11.5 Å) and Na-Mag (15.5 Å), indicating the intercalation of polymolybdate species into the interlayer of magadiite. The sizes of the interlayer polymolybdate species can be estimated to be ~6.9 Å (11.5−18.4 Å) along the *c*-axis direction, while some particles found in the layered magadiite by TEM observation were <2 nm in size (see Figure 5). In

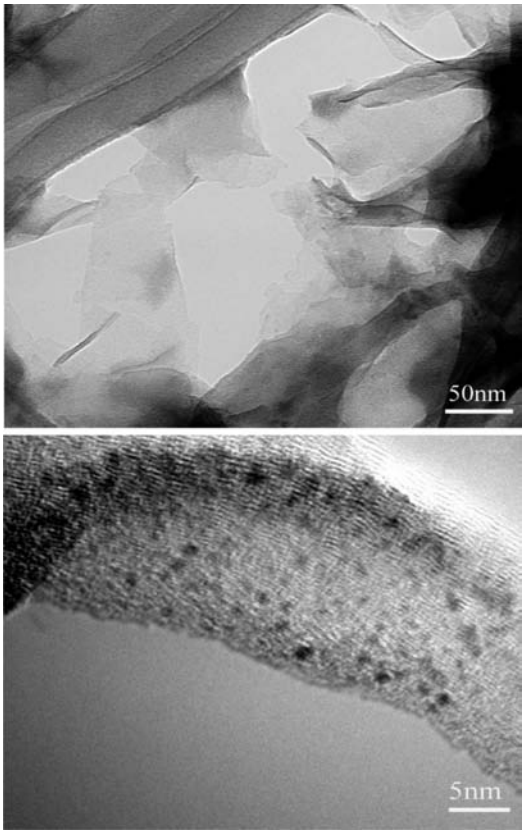

Figure 5. TEM observation of the polymolybdate/Mag composite.

general, the size of the interlayer polymolybdate species may be very small along the *c*-axis direction due to the confinement of layers, while along the direction parallel to layers, the size of interlayer polymolybdate species may be larger. This provides a reason for the different sizes based on TEM observations and the calculated value from interlayer spacing based on XRD measurement. Except for some reflections (indexed) attributed to H-Mag phase, other reflections (assigned as •) are matched with $Na_4Mo_8O_{26}\cdot 12H_2O$ [PDF No. 35-1465].[18] It is noticeable that the interlayer polymolybdate species should not be the

dx.doi.org/10.1021/ic400569y | Inorg. Chem. 2013, 52, 7431−7440

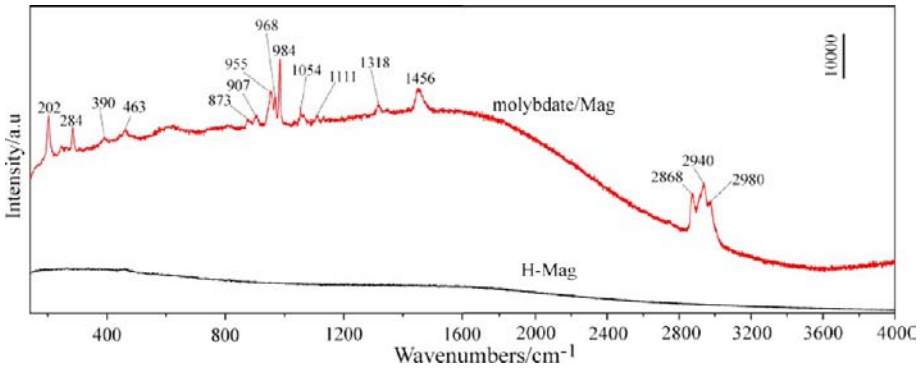

Figure 6. Raman spectroscopy of H-Mag and polymolybdate/Mag.

$Na_4Mo_8O_{26}\cdot 12H_2O$ phase, because there are no Na signals present in the EDX spectrum (Figure 1). In general, if the topology is very similar between the $Na_4Mo_8O_{26}\cdot 12H_2O$ and the new polymolybdate species, some reflections that originated from them may be overlapping. Therefore, the new polymolybdate species may be $(TBA)_xH_{4-x}Mo_8O_{26}$, based on the above analyses of the composition and reaction system. The nature of the new polymolybdate species was further supported by Raman spectroscopy.

Raman Spectroscopy. Raman spectra of H-Mag and polymolybdate/Mag are shown in Figure 6. For the polymolybdate/Mag composite, the bands can be assigned as follows: 955–984 cm^{-1} bands, Mo═O stretching modes; 873–907 cm^{-1} bands, asymmetric Mo–O–Mo stretches; 390–463 cm^{-1} range, symmetric Mo–O–Mo stretches, and ~206 and 284 cm^{-1}, Mo–O–Mo deformations.[10a] The Raman spectroscopy revealed main peaks at 984, 968, 955 cm^{-1}, along with small peaks at 907, 873, and 463 cm^{-1}. These peak positions matched neither the MoO_4^{2-} ions nor the $Mo_7O_{24}^{6-}$ ions in acidic solution, but were close to those of solid $(NH_4)_4Mo_8O_{26}\cdot 4H_2O$.[10a] The bands at 1054, 1111, 1318, 1456, 2868, 2940, and 2980 cm^{-1} were attributed to tetra-*n*-butylammonium.[19] Based on the above analysis, the polymolybdate species incorporated in the magadiite should be $Mo_8O_{26}^{4-}$. These results are consistent with the compositional analyses.

Thermal Analysis. TG curves of Na-Mag, H-Mag, and polymolybdate/Mag are shown in Figure 2. As shown in TG curves, Na-Mag showed a typical interlayer water loss up to 280 °C. Rapid mass loss up to 145 °C was followed by slower mass loss, approaching a constant value toward the end of thermal dehydration at 280 °C. At this temperature, a mass loss of 12.4% was observed.[11] H-Mag exhibited an initial weight loss of 1.2% at temperatures below 300 °C, because of the desorption of H_2O. The 1.7% weight loss in the temperature range of 300–400 °C was attributed to the elimination of OH groups from the structure. This behavior of thermal decomposition was similar in existing literature.[20] The thermal decomposition of polymolybdate/Mag was different from those of Na-Mag and H-Mag. Four mass loss steps, represented in temperature ranges of 25–100 °C, 100–235 °C, 235–490 °C, and 490–800 °C, can be recorded. This behavior of thermal decomposition was analogous to that containing the $Mo_8O_{26}^{4-}$ composite.[11a]

XPS Analyses. To confirm the nature of the polymolybdate, the chemical states of Mo 3d and O 1s have been analyzed by XPS. For the as-prepared polymolybdate/Mag (Figure 7), following the survey scan, high-resolution XPS spectra of the C 1s, O 1s, Si 2p, and Mo 3d energy levels were recorded. The

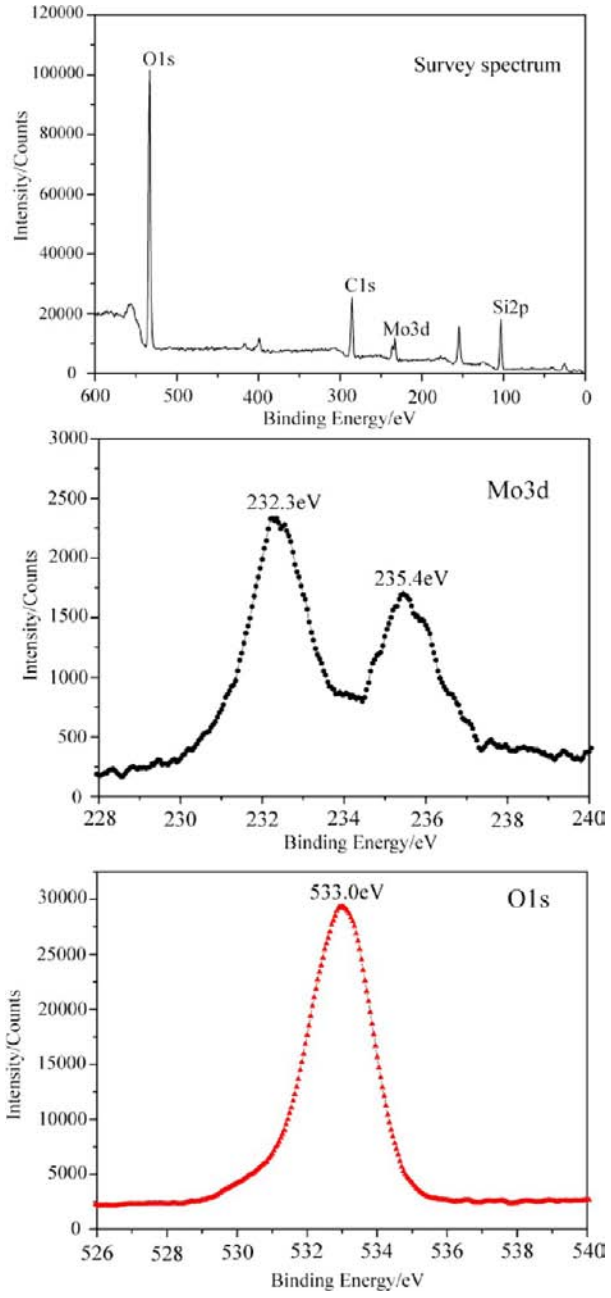

Figure 7. XPS survey spectrum of polymolybdate/Mag sample and the Mo and O elemental electronic spectra.

dx.doi.org/10.1021/ic400569y | *Inorg. Chem.* 2013, 52, 7431–7440

spectrum of the as-prepared polymolybdate/Mag composite in the Mo 3d region showed the presence of two well-resolved spectral lines at 232.3 and 235.4 eV, which were assigned to the Mo $3d_{5/2}$ and Mo $3d_{3/2}$ spin−orbit components, respectively. The binding energy of the Mo $3d_{5/2}$ line for Mo(VI) in molybdenum oxide has been reported to be 232.2−232.6 eV.[21] While the spin-orbit splitting of the Mo 3d level in molybdate or polymolybdate for the +6 oxidation state often gives rise to two deconvoluted peaks at binding energies of BE = 233.4 eV and BE = 236.5 eV, respectively,[21] and the +5 oxidation state often gives rise to peaks at 231.9 eV and 235.0 eV.[21a,22] The present Mo 3d spectrum contains strong peaks at 232.3(Mo $3d_{5/2}$) and 235.4 eV (Mo $3d_{3/2}$), which are between those of the Mo^{6+} and Mo^{5+} state. This peak position value between +5 and +6 state in the polymolybdate/Mag may be caused by photochromism during XPS measurement since the color of the sample changed only slightly after the XPS measurement. Winograd et al. had observed the photochromism of the ammonium molybdate during XPS measurement.[21a] The O 1s peak at 533.0 eV was associated with the O atoms in silicate and the O atoms in stoichiometric MoO_3.[23] All the results further supported the nature of polymolybdate enclosed in magadiite.

On the basis of the CHN elemental analysis, SEM-EDX compositional analysis, TG, Raman spectroscopy, XPS, and XRD, we conclude that polymolybdate species enclosed in the magadiite is $Mo_8O_{26}^{4-}$.

Photochemistry of Polymolybdate/Mag. Polymolybdate/Mag powders were put into a round groove of a sample support and pressed tightly. The sample with a diameter of 0.5 in. and a thickness of 3.0 mm was illuminated with visible light (420−630 nm) from a 300 W mercury arc lamp in air. The light intensity irradiating the samples was determined to be 1.0−5.0 mW/cm^2. Figure 8 shows the UV−vis diffuse reflectance spectra of the polymolybdate/Mag sample with different irradiating power. As shown in Figure 8, the as-prepared polymolybdate/Mag (yellow) exhibited a strong UV absorption peak at ∼250 nm. Upon visible-light irradiation for 15 min with power of 1.0 mW/cm^2, the UV absorption decreased markedly, and a new visible absorption at ∼500 nm was observed. With increasing irradiation power, the UV absorption continued to decrease and the visible absorption increased. The UV absorption corresponds to the charge transfer from an O^{2-} ion to a Mo^{6+} ion, and the visible absorption (500 nm) corresponds to the charge transfer from an O^{2-} ion to a Mo^{5+} ion. With increasing irradiating power, more of the Mo^{6+} state ions were reduced to the Mo^{5+} state, leading to an increase in visible absorption (500 nm) and a decrease in UV absorption. When the irradiating power was increased to 3.0 mW/cm^2, the visible absorption (500 nm) saturated, suggesting that the reduction of all of the surface Mo^{6+} state to the Mo^{5+} state, because the irradiation was mainly on the surface of the sample. The visible absorption peak shifted slightly, to 490 nm, as the irradiating power increased up to 5.0 mW/cm^2. Figure 9 shows photographic images: the yellow as-prepared sample became green-blue as it was exposed to visible-light irradiation, and then the green-blue color turned into blue and dark blue as the irradiation power increased.

The UV−vis diffuse reflectance spectra of the polymolybdate/Mag sample, as a function of irradiating time, are shown in Figure 10. A strong UV absorption peak at 250 nm was found in the as-prepared polymolybdate/Mag. Upon visible-light irradiation for 10 min with a power of 3.0 mW/cm^2, the UV

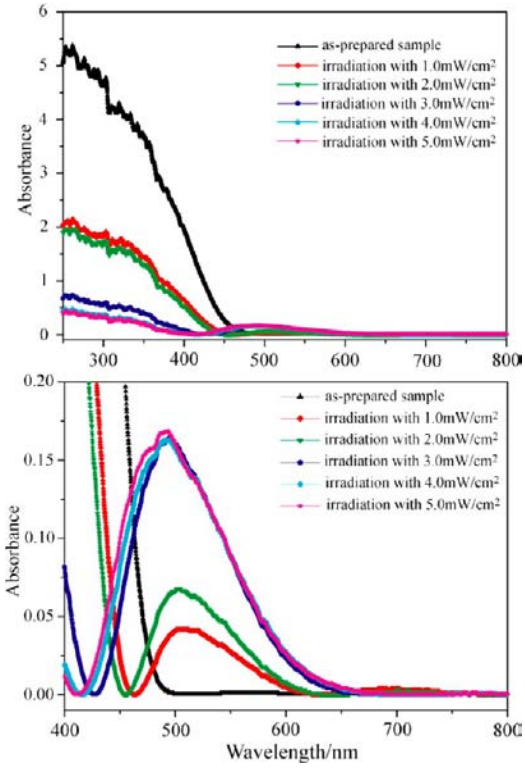

Figure 8. UV−vis diffuse reflectance spectra of the polymolybdate/Mag composite dependence on irradiating power, using an irradiating time of 15 min.

absorption decreased markedly and a new visible absorption at ∼500 nm was observed. The UV absorption then continued to decrease and the visible-light absorption increased as the irradiation time increased. Moreover, the visible absorption peak also shifted slightly, to 490 nm, as the irradiating time increased up to 40 min. It is worthwhile to notice that no band between 600 nm and 800 nm was observed in any of the samples, which is often found in some organic hybrids that contain $Mo_8O_{26}^{4-}$.[2a,11f] However, similar maximum visible-light absorbance or Kubelka−Munk transformed reflectivity were found at ∼473, 500, or 510 nm in some composites containing polymolybdate or polytungstate.[24] This may be due to the photochromic mechanism of polymolybdate.

The reversibility of the colored samples was examined by H_2O_2 bleaching (see Figure 11). After bleaching, the irradiation was repeated. All the bleaching was done with 15% H_2O_2 solution. The blue color faded quickly (within 2 min) in every bleaching reaction. The experiment was carried out on two consecutive days, and with five bleaching/photolysis cycles each day. Figure 11 shows the visible-light absorption spectra of colored and bleached samples. In the first day, the bleaching was carried out by 15% H_2O_2 solution, and five cycles (1−5 times) of bleaching−irradiation were completed. The maximum absorption of colored samples was almost similar in every cycle. The next day, the sample was further subjected to 6−10 cycles. During this experiment, the bleaching also employed a 15% H_2O_2 solution. We found that the maximum absorption of colored samples was almost unchanged from the first cycle to the tenth cycle, suggesting a good reversibility of photochromism for the polymolybdate/Mag composite. In addition, the yellow sample gradually turned pale yellow after being bleached in several cycles (see Figure 12). This may be due to

dx.doi.org/10.1021/ic400569y | Inorg. Chem. 2013, 52, 7431−7440

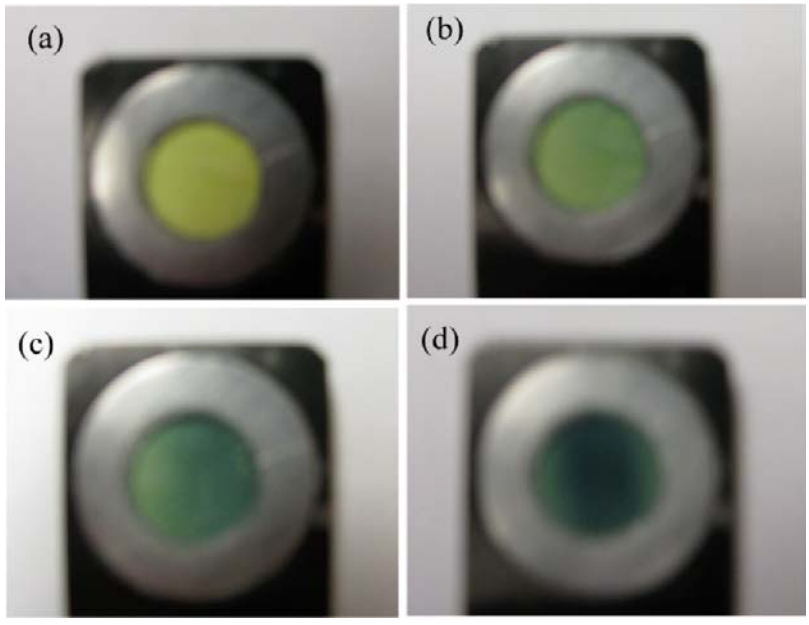

Figure 9. Coloration pictures of (a) the as-prepared polymolybdate/Mag composite and (b–d) the polymolybdate/Mag composite irradiated at (b) 1.0 mW/cm^2, (c) 3.0 mW/cm^2, and (d) 5.0 mW/cm^2, respectively, for 15 min.

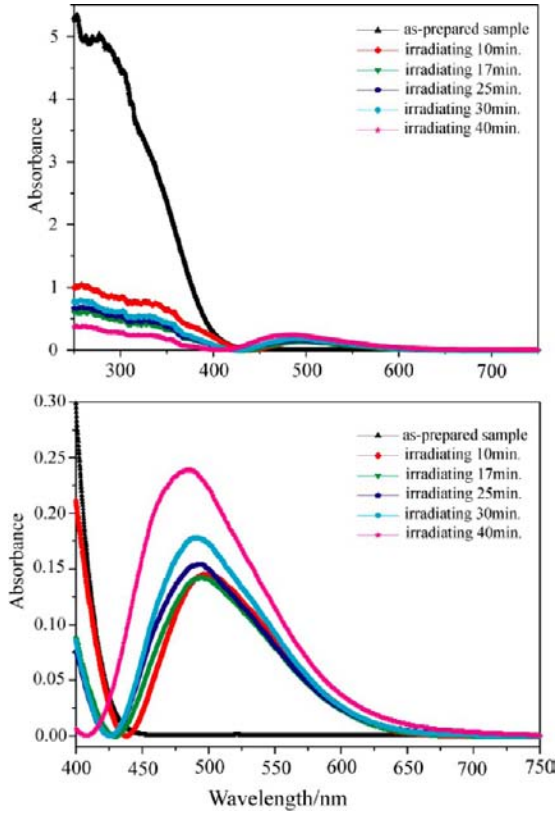

Figure 10. UV–vis diffuse reflectance spectra of the polymolybdate/Mag composite, depending on irradiating time under an irradiation power of 3.0 mW/cm^2.

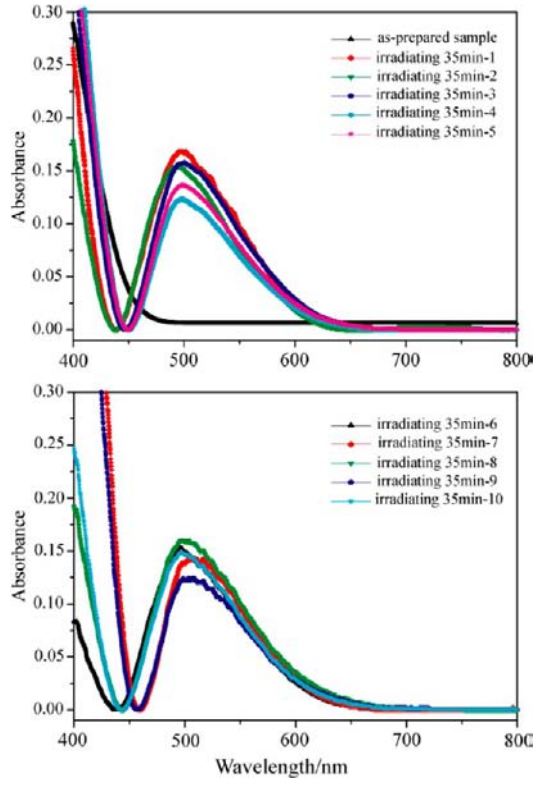

Figure 11. Reversibility of coloration–decoloration for polymolybdate/Mag for 1–10 times.

the bleaching property of H_2O_2 solution. Although the bleached sample cannot recover its original yellow color, the bleached sample can be colored (blue) again when irradiated by visible light.

Mechanism of Photochromism. For MoO_3, most studies suggest that oxygen vacancies and water molecules play an important role in photochromism.[4] Since the as-prepared MoO_3 often contain water on the surface or interior, the necessary protons for the coloration can be generated from the reaction of the adsorbed water with holes. Subsequently the protons produced can diffuse into the MoO_3 lattice to combine with MoO_3, forming hydrogen molybdenum bronze $H_xMo^{V}_xMo^{VI}_{1-x}O_3$. Meanwhile, the Mo^{6+} captures an adjacent electron, becoming Mo^{5+}, which is the photochromic core; as a

dx.doi.org/10.1021/ic400569y | Inorg. Chem. 2013, 52, 7431–7440

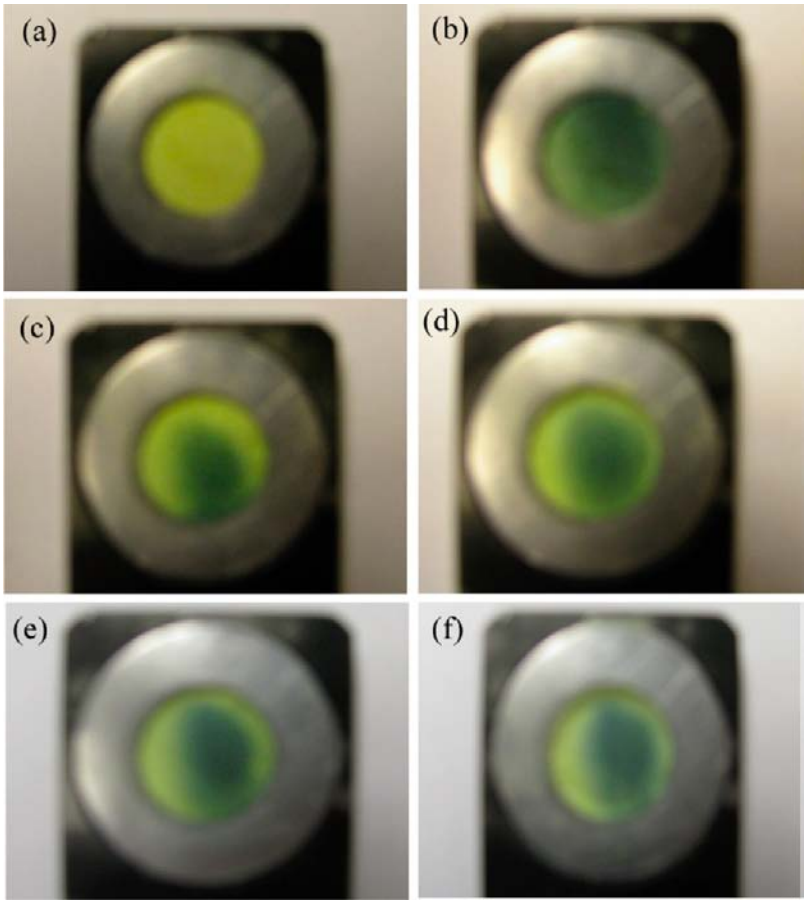

Figure 12. Pictures of (a) the as-prepared polymolybdate/Mag and the (b) first-time coloration, (c) third-time coloration, (d) fifth-time coloration, (e) seventh-time coloration, and (f) tenth-time coloration.

result, the powder turns blue, because of the intervalence-charge transfer from the newly formed Mo^{5+} (valence band) to the adjacent Mo^{6+} (conduction band). The reaction proceeds as follows:[4]

$$MoO_3 + h\nu \rightarrow MoO^* + e^- + h^+$$

$$h^+ + \frac{1}{2}H_2O \rightarrow H^+ + \frac{1}{4}O_2$$

$$MoO_3 + xe^- + xH^+ \rightarrow H_xMo^{V}{}_xMo^{VI}{}_{1-x}O_3$$

With regard to polymolybdate, it can be seen as metal-oxide clusters, because of the similar composition and topology between isopolymolybdate and molybdenum.[25] Similar to the behavior of semiconducting molybdenum oxides, polyoxomolybdates can be photochemically reduced to form colored mixed-valence species by UV-light irradiation.[26] During the reduction reaction, the coloration was attributed to a transfer of the proton involved in the hydrogen bond between anions and organic cations or organic ligands, such as alkylammonium, alcohols, carboxylic acids, etc. However, few polyoxometalates exhibit perfect reversibility of the coloration.[25] The irreversibility of the color change arises from an uncharacterized side reactions during both the coloration and decoloration of the polyoxometalates.

Comparably, the present polymolybdate/Mag composite based on $(TBA)_xH_{4-x}Mo_8O_{26}$ enclosed in magadiite showed coloration under visible-light irradiation, and irradiation can be repeated many times. No H atom was bonded with N atoms in the TBAOH, that is, TBA^+ present the composite does not play a role in photochromism. Therefore, the photochromic mechanisms of the composite may be different from those of above-mentioned polyoxomolybdates. Based on an extension of the above-mentioned principles as well as photochromic mechanisms of molybdenum oxide and other polymolybdates,[4,25,26] the photochromic mechanism of the present composite may be explained as follows:

$$[Mo^{VI}{}_8O_{26}]^{4-}(\text{yellow}) + h\nu \rightarrow [Mo^{VI}{}_8O_{26}]^{4-*} \quad (1)$$

$$[Mo^{VI}{}_8O_{26}]^{4-*} + H_2O \rightarrow [HMo^{VI}{}_7Mo^{V}O_{26}]^{4-}(\text{blue}) + \bullet OH \quad (2)$$

When $(TBA)_xH_{4-x}Mo_8O_{26}$ powder was irradiated with visible light, a photochemically active species $[Mo^{VI}{}_8O_{26}]^{4-*}$ was formed. The active species $[Mo^{VI}{}_8O_{26}]^{4-*}$ then can be reduced by water splitting under photoirradiation, becoming $[HMo^{VI}{}_7Mo^{V}O_{26}]^{4-}$ and thus producing hydroxyl radicals (•OH). Therefore, the interlayer water molecules of magadiite present in the polymolybdate/Mag composite play a key role in the coloration of the composite. There are some reports on hydrogen-bond interaction between interlayer water or guests and the layers in magadiite;[12] it is highly possible that hydrogen bonding exists between the interlayer hydroxyl groups of magadiite or interlayer water molecule and interlayer $Mo_8O_{26}{}^{4-}$ species in the composite. Although most studies on photochromic $Mo_8O_{26}{}^{4-}$ materials reported that the charge carrier

dx.doi.org/10.1021/ic400569y | Inorg. Chem. 2013, 52, 7431−7440

needs a strong UV excitation, because of its very high energetic oxygen-to-molybdenum charge transfers into this cluster, the hydrogen bond between water molecules and $Mo_8O_{26}^{4-}$ or the terminal O atom present in the composite weaken the O−H bond of H_2O and make the water splitting easier, leading to the facile reduction of the $Mo_8O_{26}^{4-}$ species. Moreover, the host magadiite has good hydration properties and can store and supply enough water molecules for the color cycling. When the sample was bleached with H_2O_2 solution, on the one hand, H_2O_2 oxidized Mo^{5+} into Mo^{6+}; in addition, the H_2O_2 solution provided enough water to compensate for the loss of water molecules during the irradiation cycle. This may be the main reason that the polymolybdate/Mag can turn blue under visible-light irradiation and the irradiation−bleaching cycle can be repeated many times. The bleaching reaction can be concluded as

$$[HMo^{VI}{}_7Mo^{V}{}_1O_{26}]^{4-}(\text{blue}) + \frac{1}{2}H_2O_2 \rightarrow [Mo^{VI}{}_8O_{26}]^{4-}(\text{yellow}) + H_2O$$

CONCLUSION

In short, a new composite-based polymolybdate enclosed in magadiite has been developed through protonation, intercalation, and exfoliation/self-assembly processing. A well-ordered phase exhibited a larger basal spacing of 18.4 Å than those of its precursors (H-Mag and Na-Mag). The nature of the polymolybdate was confirmed by X-ray diffraction (XRD), Raman spectroscopy, and X-ray photoelectron spectroscopy (XPS), as well as reaction system analyses. The photochromism of polymolybdate/Mag was investigated in detail. The yellow as-prepared sample turned green-blue as it was exposed to visible-light irradiation, then further turned blue and dark blue as the irradiation power or time increased.

The reversibility of the colored samples can be realized by bleaching with a 15% H_2O_2 solution. After bleaching, the irradiation can be repeated. When the bleaching (decoloration) was done with a 15% H_2O_2 solution, the blue color faded quickly (within 2 min). The coloration−decoloration cycles can be repeated in excess of 10 times, although the bleached sample cannot recover the original yellow color, nevertheless, a more pale yellow is produced. This material exhibits good visible-light photochromic reversibility, making it potentially useful in the photochromic applications, such as optical signal processing and smart windows. Moreover, this material should have higher thermal stability, in comparison with those of organic or inorganic−organic photochromic materials.

AUTHOR INFORMATION

Corresponding Author

*Tel.: 86-0791-83969514. Fax: 86-0791-83969514. E-mail: yfchen@ncu.edu.cn.

Notes

The authors declare no competing financial interest.

ACKNOWLEDGMENTS

This project was supported by the National Natural Science Foundation of China (Grant No. 51162021). The authors thank Dr. Prabir Dutta (Department of Chemistry, The Ohio State University) for providing the measurement of photochromism and Raman spectra.

REFERENCES

(1) (a) Arnaud-Neu, F.; Schwing-Weill, M. J. *J. Less-Common Met.* **1974**, *36*, 71−78. (b) Shallcross, R. C.; Zacharias, P.; Köhnen, A.; Körner, P. O.; Maibach, E.; Meerholz, K. *Adv. Mater.* **2013**, *25*, 469−476. (c) Weber, C.; Rustemeyer, F.; Dürr, H. *Adv. Mater.* **1998**, *10*, 1348−1351. (d) Tomasulo, M.; Sortino, S.; Sortino, F. M. *Adv. Mater.* **2008**, *20*, 832−835. (e) Singer, M.; Jäschke, A. *J. Am. Chem. Soc.* **2010**, *132*, 8372−8377.

(2) (a) Dessapt, R.; Collet, M.; Coué, V.; Bujoli-Doeuff, M.; Jobic, S.; Lee, C.; Whangbo, M. H. *Inorg. Chem.* **2009**, *48*, 574−580. (b) Hakouk, K.; Oms,, O.; Dolbecq, A.; Moll, H. E.; Marrot, J.; Evain, M.; Molton, F.; Duboc, C.; Deniard, P.; Jobic, S.; Mialane, P.; Dessapt, R. *Inorg. Chem.* **2013**, *52*, 555−557. (c) Li, B.; Wang, J. Y.; Wen, H. M.; Shi, L. X.; Chen, Z. N. *J. Am. Chem. Soc.* **2012**, *34*, 16059−16067. (d) Leblanc, N.; Bi, W. H.; Mercier, N.; Auban-Senzier, P.; Pasquier, C. *Inorg. Chem.* **2010**, *49*, 5824−5833. (e) Lv, X. Y.; Wang, M. S.; Yang, C.; Wang, G. E.; Wang, S. H.; Lin, R.; Guo, G. C. *Inorg. Chem.* **2012**, *51*, 4015−4019.

(3) (a) Yamase, T.; Hayashi, H.; Ikawa, T. *Chem. Lett.* **1974**, 1055−1056. (b) Yamase, T.; Ikawa, T. *Bull. Chem. Soc. Jpn.* **1977**, *50*, 746−749. (c) Yamase, T. *J. Chem. Soc., Dalton Trans.* **1978**, 283−285. (d) Yamase, T.; Ikawa, T.; Kokado, H.; Inoue, E. *Chem. Lett.* **1973**, 615−616.

(4) (a) Shen, Y.; Huang, R.; Cao, Y. Y.; Wang, P. P. *Mater. Sci. Eng., B* **2010**, *172*, 237−241. (b) He, T.; Yao, J. N. *J. Photochem. Photobiol. C: Photochem. Rev.* **2003**, *4*, 125−143. (c) Yan, M. Y.; Shen, Y.; Zhao, L.; Li, Z. *Mater. Res. Bull.* **2011**, *46*, 1648−1653.

(5) (a) Eypert-Blaison, C.; Humbert, B.; Michot, L. J.; Pelletier, M.; Sauzéat, E.; Villiéras, F. *Chem. Mater.* **2001**, *13*, 4439−4446. (b) Aline, O. M.; Alexandre, G. S. P. *J. Colloid Interface Sci.* **2009**, *330*, 392−398. (c) Eypert-Blaison, C.; Sauzéat, E.; Pelletier, M.; Michot, L. J.; Villiéras, F.; Humbert, B. *Chem. Mater.* **2001**, *13*, 1480−1486.

(6) Brandt, A.; Schwieger, W.; Bergk, K. H. *Cryst. Res. Technol.* **1988**, *23*, 1201−1203.

(7) (a) Guerra, D. L.; Pinto, A. A.; Airoldi, C.; Viana, R. R. *J. Solid State Chem.* **2008**, *181*, 3374−3379. (b) Wang, Z.; Pinnavaia, T. J. *J. Mater. Chem.* **2003**, *13*, 2127−2131. (c) Petrucelli, G. C.; Meirinho, M. A.; Macedo, T. R.; Airoldi, C. *Thermochim. Acta* **2006**, *450*, 16−21. (d) Díaz, U.; Cantín, Á.; Corma, A. *Chem. Mater.* **2007**, *19*, 3686−3693. (e) Yukutake, H.; Kobayashi, M.; Otsuka, H.; Takahara, A. *Polymer J.* **2009**, *41*, 555−561. (f) Takahashi, N.; Kuroda, K. *J. Mater. Chem.* **2011**, *21*, 14336−14353.

(8) (a) Gould, D. M.; Spiro, M.; Griffith, W. P. *J. Mol. Catal. A.* **2005**, *234*, 145−150. (b) Gould, D. M.; Griffith, W. P.; Spiro, M. *J. Mol. Catal. A* **2001**, *175*, 289−291.

(9) Okwon, O. Y.; Jeong, S. Y.; Suh, J. K.; Lee, J. M. *Bull. Korean Chem. Soc.* **1995**, *16*, 737−742.

(10) (a) Griffith, W. P.; Lesniak, P. J. B. *J. Chem. Soc. (A)* **1969**, 1066−1071. (b) Mahadevaiah, N.; Venkataramani, B.; Jai Prakash, B. S. *Chem. Mater.* **2007**, *19*, 4606−4612. (c) Aveston, J.; Anacker, E. W.; Johnson, J. S. *Inorg. Chem.* **1964**, *3*, 735−746.

(11) (a) Shen, E. H.; Lu, J.; Li, Y. G.; Wang, E. B.; Hu, C. W.; Xu, L. *J. Solid State Chem.* **2004**, *177*, 4372−4376. (b) Simonng, K. Y.; Gulari, E. *Polyhedron* **1984**, *3*, 1001−1011. (c) Bridgeman, A. J. *J. Phys. Chem. A* **2002**, *106*, 12151−12160. (d) Mooney, W.; Chauveau, F.; Tran-Thi, T. H.; Folche, G. *J. Chem. Soc., Perkin Trans. II* **1988**, 1479−1484. (e) Zhang, G. J.; Dong, X. Y.; Yang, W. S.; Yao, J. N. *Thin Solid Films* **2006**, *496*, 533−538. (f) Yamase, T.; Kurozumi, T. *J. Chem. Soc., Dalton Trans.* **1983**, 2205−2209. (g) Wang, W. J.; Xu, L.; Wei, Y. G.; Li, F. Y.; Gao, G. G.; Wang, E. B. *J. Solid State Chem.* **2005**, *178*, 608−612. (h) Lan, Y. Q.; Li, S. L.; Wang, X. L.; Shao, K. Z.; Su, Z. M.; Wang, E. B. *Inorg. Chem.* **2008**, *47*, 529−534.

(12) (a) Macedo, T. R.; Claudio Airoldi, C. *Microporous Mesoporous Mater.* **2006**, *94*, 81−88. (b) Almond, G. G.; Harris, R. K.; Graham, P. *J. Chem. Soc., Chem. Commun.* **1994**, 851−852. (c) Komori, Y.; Miyoshi, M.; Hayashi, S.; Sugahara, Y.; Kuroda, K. *Clays Clay Miner.* **2000**, *48*, 632−637. (d) Rojo, J. M.; Ruiz-Hitzky, E.; Sanz, J. *Inorg. Chem.* **1988**, *27*, 2785−2790. (e) Wang, X. Q.; Liu, L. M.; Huang, J.; Jacobson, A. J. *J. Solid State Chem.* **2004**, *177*, 2499−2505.

(13) Aline, O. M.; Alexandre, G.S. P. *J. Colloid Interface Sci.* **2009**, *330*, 392−398.
(14) (a) Garces, J. M.; Rocke, S. C.; Crowder, C. E.; Hasha, D. L. *Clays Clay Miner.* **1988**, *36*, 409−418. (b) Lagaly, G.; Beneke, K.; Weiss, A. *Am. Mineral.* **1975**, *60*, 642−649.
(15) (a) Fethi, K.; Liu, Y. *J. Phys. Chem. C* **2009**, *113*, 1947−1952. (b) Peng, S. G.; Gao, Q. M.; Du, Z. L.; Shi, J. L. *Appl. Clay Sci.* **2006**, *31*, 229−237.
(16) (a) Pastore, H. O.; Munsignatti, M.; Mascarenhas, A. J. S. *Clays Clay Miner.* **2000**, *48*, 224−229. (b) Dailey, J. S.; Pinnavaia, T. J. *Chem. Mater.* **1992**, *4*, 855−863.
(17) Schwieger, W.; Heidemann, D.; Bergk, K. H. *Rev. Chim. Miner.* **1985**, *22*, 639−650.
(18) Rich, H.; Fuchs, Z. *Naturforsch., B: Anorg. Chem. Org. Chem.* **1984**, *39*, 623−627.
(19) (a) Hashimoto, S.; Sugahara, T.; Moritoki, M.; Sato, H.; Ohgaki, K. *Chem. Eng. Sci.* **2008**, *63*, 1092−1097. (b) Oshima, M.; Shimada, W.; Hashimoto, S.; Tani, A.; Ohgaki, K. *Chem. Eng. Sci.* **2010**, *65*, 5442−5446.
(20) Macedo, T. R.; Petrucelli, G. C.; Airoldi, C. *Clays Clay Miner.* **2007**, *55*, 151−159.
(21) (a) Ilangovan, G.; Pillai, K. C. *Langmuir* **1997**, *13*, 566−575. (b) Grunert, W.; Stakheev, A. Y.; Feldhaus, R.; Anders, K.; Shpire, E. S.; Minachev, K. M. *J. Phys. Chem.* **1991**, *95*, 1323−1328. (c) Clayton, C. R.; Lu, Y. C. *Surf. Interface Anal.* **1989**, *14*, 66−70.
(22) Uchida, K.; Ayame, A. *Surf. Sci.* **1996**, *357*−*358*, 170−175.
(23) (a) Gedeon, O.; Zemek, J.; Jiricek, P. *Nucl. Instr. Meth. B* **2012**, *280*, 111−116. (b) Xie, F. Y.; Gong, L.; Liu, X.; Tao, Y. T.; Zhang, W. H.; Chen, S. H.; Meng, H.; Chen, J. *J. Electron Spectrosc. Relat. Phenom.* **2012**, *185*, 112−118.
(24) (a) Dessapt, R.; Gabard, M.; Bujoli-Doeuff, M.; Deniard, P.; Jobic, S. *Inorg. Chem.* **2011**, *50*, 8790−8796. (b) Chen, Y. F.; Yu, G. S.; Li, F.; Xie, C. F.; Tian, G. P. *J. Mater. Chem. C* DOI: 10.1039/c3tc30309h. (c) Wu, Q. Y.; Wang, H. B.; Yin, C. S.; Meng, G. Y. *Mater. Lett.* **2001**, *50*, 61−65.
(25) Yamase, T. *Chem. Rev.* **1998**, *98*, 307−325.
(26) (a) Papaconstantinous, E. *Chem. Soc. Rev.* **1989**, *18*, 1−31. (b) Yamase, T. *Catal. Surv. Asia* **2003**, *7*, 203−216. (c) Yamase, T.; Kurozumi, T. *Inorg. Chim. Acta* **1984**, *83*, L25−L27. (d) Yamase, T.; Kurozumi, T. *J. Chem. Soc., Dalton Trans.* **1983**, 2205−2209. (e) Li, D.; Yuranova, T.; Albers, P.; Kiwi, J. *Water Res.* **2004**, *38*, 3541−3550. (f) Kraut, B. *J. Photochem. Photobiol. A: Chem.* **1992**, *68*, 107−113.